NeuroImage **16,** 801–813 (2002)
doi:10.1006/nimg.2002.1116

Efficient Design of Event-Related fMRI Experiments Using M-Sequences

Giedrius T. Buračas and Geoffrey M. Boynton

SNL-B, Salk Institute, La Jolla, California 92037

Received October 23, 2001

Rapid event-related fMRI (erfMRI) allows estimation of the shape of hemodynamic responses (HDR) associated with transient brain activation evoked by various sensory, motor, and cognitive events. Choosing a sequence of events that maximizes efficiency of estimating the HDR is essential for conducting event-related brain imaging experiments, since increasing efficiency is essentially equivalent to reducing scanning time or increasing the strength of the principal magnetic field. The efficiency of an erfMRI design depends critically on the temporal arrangement of the sequence of events and the noise in the fMRI signal. We introduce to erfMRI a simple method for generating efficient event sequences based on maximum-length shift register sequences, or m-sequences. We show that under the assumption of white uncorrelated MRI noise, efficiency of erfMRI experimental designs that employ m-sequences exceeds efficiency of the best randomly generated sequences. This is true for single and multiple event type experiments, which allow either parallel events (overlapping events design) or designs in which only one event occurs at a time (nonoverlapping events design). HDR estimation efficiency afforded by m-sequences grows with the number of event types, and is greatest when event sequences are relatively short, albeit within commonly used scan times (i.e., 63–255 total events per scan). The improvement in efficiency, however, comes at a cost of constraints imposed by m-sequence generation rules, such as predetermined sequence lengths; for nonoverlapping events design m-sequence-based designs are not available for all possible numbers of event types. Nevertheless, designs that are available with m-sequences cover a large subset of commonly used erfMRI experimental designs. Under conditions of characteristic time-correlated fMRI noise, randomly generated sequences may yield efficiencies that exceed those afforded by m-sequences for single event-type designs, since in this case one can generate random sequences that partially decorrelate MRI noise by chance. Our simulations suggest that for designs of realistic sequence lengths that use more than one event type, m-sequence based designs tend to outperform random designs, thus making the knowledge of noise inessential. Finally, within an *r*-th order m-sequence (generated by a shift register of length *r*) all possible combinations of subsequences of length *r* occur, and thus these subsequences are exactly counterbalanced. This property is essential for minimizing effects of psychological and neuronal adaptation and expectation.

INTRODUCTION

During last few years, rapid event-related designs (erfMRI) have become a predominant paradigm for fMRI experiments. The appeal of erfMRI stems from its ability to resolve hemodynamic responses (HDR) associated with transient neural activity caused by multiple types of stimuli and/or cognitive tasks. Unlike the traditional block design paradigm that strings identical event types together in a row, event-related fMRI (erfMRI) allows for different event types to be interleaved in an arbitrary manner (e.g., Burock *et al.*, 1998; Rosen *et al.*, 1998; Hinrichs *et al.*, 2000). Most importantly, while the block design is optimal for detecting activity in the brain, event-related fMRI is optimal for estimating the parameters of the HDR associated with individual events (e.g., Friston *et al.*, 1999; Liu *et al.*, 2001).

The estimation efficiency of a given event-related sequence is a mathematical construct that reflects the ability of the sequence to provide an estimate of the HDR, taking into account noise associated with the fMRI signal (e.g., Dale, 1999). Maximization of HDR estimation efficiency is critical for erfMRI experimental design, since it minimizes the error in estimating the HDR for a data set of given size, or alternatively, reduces overall scanning time for a criterion signal-to-noise level. The significance of maximizing estimation efficiency can be further appreciated by considering the fact that increasing estimation efficiency is equivalent to increasing the strength of the main magnetic field of the scanner.

1053-8119/02 $35.00

HDR estimation efficiency depends on a number of factors including the nature of fMRI noise, scan duration, number of sampling points in the HDR estimate, and the distribution of event occurrences in time. An experimenter cannot easily control fMRI noise, but the remaining factors can be manipulated by choosing appropriate parameters in the experimental design, such as the sequence of events.

An erfMRI experiment can be designed using any arbitrary sequence of events, but estimation efficiency varies broadly for different sequences. A common method for choosing an event-related sequence is to generate a large number of random sequences and to pick the one that yields maximum estimation efficiency. While this method, in theory, will eventually produce the maximally efficient sequence of the large but finite number of possibilities, obtaining this sequence in practice can take a prohibitive amount of computational resources. Instead, we present a class of sequences, called m-sequences (maximum length shift-register sequences), which provide HDR estimation efficiency superior to that of random sequences at a very low computational cost. Another advantage of m-sequences is their ease of generation, since the number of computations grows only linearly with sequence length.

Introduced nearly half a century ago, m-sequences have been used extensively in encryption, error-correcting codes, pseudorandom sequence generation where quick generation of random sequences is needed, signal recovery from noise (e.g., Golomb, 1982), and linear system analysis (e.g., Sutter, 1987). Recently m-sequence based methods have been extended to multi-input nonlinear systems analysis, and applied to mapping receptive fields in mammalian visual system (e.g., Bernadette and Victor, 1994). Only recently have M-sequences been applied to erfMRI experiments (see, e.g., Fize *et al.*, 2000).

M-sequences maximize HDR estimation efficiency in two ways. First, the number of events is equal for all event types (including zero-events), which maximizes the number of presentations for all event types (Liu *et al.*, 2001). Second, m-sequences are nearly orthogonal to cyclically time-shifted versions of themselves. While random sequences are orthogonal to time-shifted versions of themselves with an average error of one over square root of sequence length, the orthogonality of time-shifted m-sequences has an error of only one over the sequence length (e.g., Bernadette and Victor, 1994). The gain in efficiency, however, comes at a cost of restricted design flexibility since their order and number of levels determine the m-sequence length. In addition, for m-sequence based designs with nonoverlapping-events, the number of event types is restricted to $L^n - 1$, where L is the number of m-sequence levels and n is an integer. This constraint on the number of event types does not apply to experimental designs with overlapping events.

HDR estimation efficiency depends not only on experimental design, but also on the nature of fMRI noise (Dale, 1999; Burock and Dale, 2000). We employ m-sequence-based experimental designs as a benchmark for evaluating how the efficiency of randomized designs is affected by information about the structure of realistic fMRI noise. We show that m-sequence based designs tend to be advantageous even in cases when fMRI noise is taken into account, although for single event type designs random sequences can be found that exceed m-sequence efficiency.

Furthermore, an m-sequence of length $L^r - 1$ counterbalances all sub-sequences of length r, because an m-sequence by design contains all permutations of all n-length subsequences (except for the all-zero subsequence). This attractive property is a direct consequence of near-orthogonality of cyclically shifted m-sequence. Event counterbalancing may be critical for eliminating biases induced by temporal context in either the neuronal or the hemodynamic response.

MATERIALS AND METHODS

General Linear Model of the HDR

Rapid event-related designs rest on the assumption that HDRs associated with individual events combine together in a linear fashion. This assumption has been found to be a reasonable approximation, at least for visual responses in the occipital cortex (Boynton *et al.*, 1996). This observation provides justification for a popular general linear model of the HDR response $R(t)$:

$$R(t) = \sum_{i=1}^{n_e} x_i(t) * h_i(t) + w(t), \qquad (1)$$

where $x_i(t) = \sum_{j=1}^{nEvents_i} \delta(t - t_{ij})$ is an "event function," with delta functions positioned at the occurrence times t_{ij} for event of type i (for the i-th event type there are $nEvents_i$ events), $h_i(t)$ is the hemodynamic response to the event of the i-th type ($i = 1..n_e$, where n_e is number of event types), often modeled by a Gamma function (e.g., Boynton *et al.*, 1996), and $w(t)$ is additive noise. FMRI time series usually exhibit a slow drift over a period of several minutes. This drift is not completely understood, and it is customary to remove it before further analysis by subtracting out a low-frequency component, often in the form of a linear trend. Equation (1) adequately models fMRI signal after this preprocessing step (c.f. Friston *et al.*, 1999; Liu *et al.*, 2001).

Since the response $R(t)$ is actually acquired as a set of discrete measurements spaced by fixed sampling intervals, it can be represented as a column vector R of

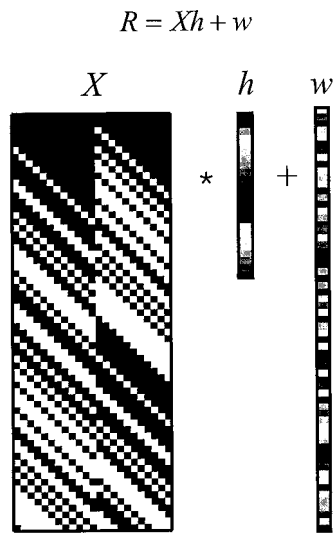

FIG. 1. Graphical representation of matrices for the general linear model. In this example two event types ($n_e = 2$) are assumed. The binary experimental design matrix X is composed of two parts, one for each event type. Each of these parts is a convolution matrix truncated at the bottom. The first column of each part corresponds to the event vector for one of event types. The vector h is composed of two concatenated HDR functions, one for each event type. Then a noise vector w is added to the result of multiplication of X and h.

size $n \times 1$. The convolution operation in the above equation can then be represented as multiplication of a HDR column vector h ($n_h n_e \times 1$) and "design matrix" X ($n \times n_h n_e$),

$$R = Xh + w, \tag{2}$$

where n_h is the number of time-samples in each hemodynamic response (Fig. 1). Note, that in the case of more than one event type ($n_e > 1$), the HDR vector h is formed by concatenating, column wise, individual (sampled) HDR responses to each event type $h = [h_1^T\ h_2^T \ldots h_{n_e}^T]^T$, and the design matrix X is a horizontal concatenation of matrices representing truncated convolution matrices for each event type: $X = [X_1\ X_2 \ldots X_{ne}]$ (e.g., Dale, 1999; see Fig. 1). For each event the HDR vector length n_h depends on the assumed duration of HDR response (typically 15–25 s), and the sampling rate.

The contribution due to noise, w, is a column vector of size ($n \times 1$) and has a covariance matrix C_n. Since fMRI noise is correlated in time, the noise is frequently modeled by a Gauss–Markov process, i.e., it is produced by filtering independent identically distributed (i.i.d.) Gaussian noise by a linear FIR filter, which determines the autocorrelation function of the noise.

The case of canonical convolution submatrices X_i corresponds to a scanning protocol whereby $n_h - 1$ data points are acquired after the last event while the HDR response returns to the baseline activity. Note that the first column vector in X_i is identical to the event vector for event i. Subsequent column vectors are merely shifted version of the event vector. A more common approach, which is used herein, is to present events all the way up to the end of image acquisition. In this case, the design matrices X_i are truncated convolution matrices without zero padding at the end (see Fig. 1).

Estimating the HDR

For the general linear model of Eq. (2), the most efficient unbiased estimator of h is the maximum likelihood estimate (e.g., Kay, 1993). For the Gaussian noise model, this estimate minimizes the least-squared error of residuals, $e = R - X\hat{h}$ (e.g., Kay, 1993; Dale, 1999):

$$\hat{h} = (X^T C^{-1} X)^{-1} X^T C^{-1} R, \tag{3}$$

where C is noise covariance matrix. If C is known exactly, this estimator produces estimation with minimum covariance equal to

$$\mathrm{cov}(h) = C_h = (X^T C^{-1} X)^{-1}. \tag{4}$$

Since the DC level from the response R is removed before analysis, the DC level in each column of X matrix is removed as well (Liu *et al.*, 2001). This preprocessing step simplifies analysis (i.e., one does not need to have a column in the X matrix that models the DC level), and keeps the covariance matrix C_h invertible.

Dale (1999) and Burock and Dale (2000) propose estimating the noise matrix, C, in two steps. First, a least squares estimate of the HDR is calculated with assumption of independent identically distributed (i.i.d.) Gaussian noise with unit variance. This is equivalent to setting C to the identity matrix in equation 2 so that $\hat{h} = (X^T X)^{-1} X^T R$. Next, the average C matrix over voxels is calculated by creating the Toeplitz matrix from an autocorrelation function of residuals $e = R - X\hat{h}$. This may be a global average or an average taken locally over voxels within region of interest (the local estimate, however, more than the global estimate tends to result in a less biased statistical inference; see Burock and Dale, 2000). The maximum likelihood estimate of h is then calculated by inserting this estimate of C to Eq. (3). An alternative method is to fit an *a priori* function (such as an exponential) to the autocorrelation function of residuals (e.g., Burock and Dale, 2000), and use the least squares estimate of autocorrelation function in the Eq. (3). Unfortunately, estimation of the noise covariance matrix is not straightforward because noise varies both across subjects and across voxels and sessions within subjects.

Estimation Efficiency

The concept of estimation efficiency can be intuitively appreciated by comparing a mean HDR function

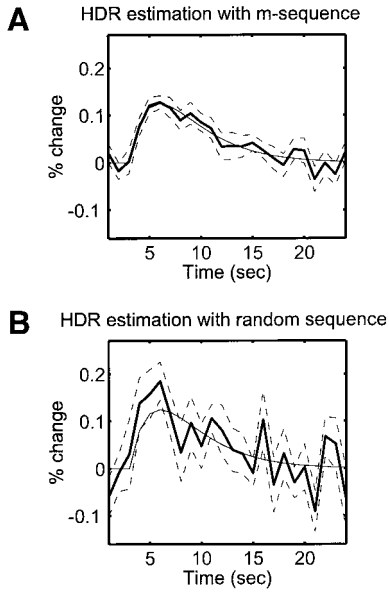

FIG. 2. Hemodynamic response functions estimated using m-sequence (A) and random sequence (B) based experimental designs. The thin smooth line indicates the original HDR function used to create simulated erfMRI response, the thick line is the mean and broken lines are standard errors of the mean. The mean and standard error were estimated from 10 repeats of a $n = 127$ interval sequence ($n_h = 24$, $n_e = 5$, SNR = 9:1). Identical noise instantiations were used in each m- and random-sequence-based HDR estimation cycle.

computed using m-sequence-based experiment (Fig. 2A) vs that computed using arbitrary random sequences (Fig. 2B). Both graphs plot the original HDR used to simulate fMRI signal (thin smooth line), mean (thick line) and standard error of the mean (broken line) estimated from simulated erfMRI experiments. The means and standard errors were obtained from 10 repeats of simulated scan across which only noise was varied (five identical event types were assumed; for clarity only the plots pertinent to the first event are plotted). The top functions were calculated using a design that employed m-sequences, and the bottom graph employed a design with random sequences. The estimated mean is much noisier in the bottom plot, and the standard error of the mean is correspondingly larger. Since the simulated noise was identical for both cases the difference in the estimation accuracy is contributable solely to the timing of events.

The notion of HDR estimation accuracy can be quantified by a scalar estimation efficiency function E, which is the inverse of the sum of the variances of the estimated HDR responses (Dale, 1999), and can be written as:

$$E = 1/trace(C_h) = 1/trace((X^T C^{-1} X)^{-1}). \quad (5)$$

According to Eq. 5, HDR estimation efficiency depends solely on the fMRI signal noise C and the design matrix X, but not on the actual shape of the HDR, h (e.g., Dale, 1999). In practice, since C cannot be known exactly, HDR estimation efficiency may depend heavily on the accuracy of the estimate of noise in the fMRI signal.

The conditions of maximum estimation efficiency for independent identically distributed (i.i.d.) Gaussian noise, $N(0,\sigma^2 1)$, were explored by Liu *et al.* (2001). In this case, $E = (\sigma^2 trace((X^T X)^{-1}))^{-1}$, where σ is the standard deviation calculated from residuals. Here the noise contribution behaves as a scaling factor, and therefore does not affect the choice of optimal design matrix X.

Efficiency depends on the probability that a given event type occurs on each trial. For example, in the case of only one event type, the condition of optimality is achieved when the probability of the event is 0.5. A second factor determining estimation efficiency is the pattern of distribution of event occurrence times within the event vector. Thus, estimation efficiency varies broadly for different random sequences that are generated using the optimal event occurrence probability.

Most importantly, random sequences that lead to optimal estimation efficiency under uncorrelated noise may be suboptimal when noise is correlated in time, as is the case with the fMRI noise. In fact, noise in the fMRI signal can be characterized by correlation times of 10–20 (e.g., Burock and Dale, 2000). The relationship between noise and design matrix becomes evident by considering the design matrix X in $C_h = (X^T C^{-1} X)^{-1}$ (c.f. Eq. (5)) as a whitening matrix that acts on the inverse of noise covariance matrix C. In other words, the design matrix, X, can serve to decorrelate the noise, C.

Generation of Random Sequences

In the simulations described below, random sequences containing identical number of events for each event type were generated using the random number generator function available in MATLAB (*The MathWorks, Inc.*). The code for generation of these sequences (function *randSequence.m* called by the function *balancedRnd.m*) is available online (see reference below).

M-Sequences

Maximum-length L level shift register sequences, or m-sequences, are pseudorandom sequences of integers that assume L different values. M-sequences are generated recurrently by a linear shift register (see Fig. 3) using modulo L arithmetic:

$$s_k = \sum_{i=1}^{r} c_i s_{k-r+i-1}, \quad (6)$$

where s_k is the next member of the sequence to be appended to the existing sequence, c_i are recurrent

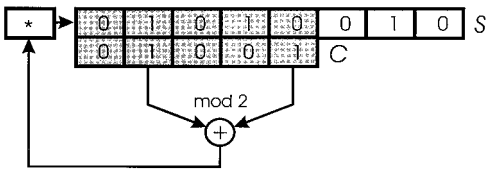

FIG. 3. Shift registers are used for generating m-sequences. In the case shown, the register (shaded component of sequence S) is composed of $r = 5$ stages, whose number determine the *order* of the m-sequence. The values in the register are weighted by weights c using modulo $L = 2$ algebra, then added together using, again, modulo 2 addition, and the result is appended to the sequence s. The register is then shifted to the left and operations repeated all over again.

coefficients, and r is the number of stages in the register, also called *the order* of a shift register. It can be shown that for an arbitrary set of weights c_i the sequence repeats itself with a period $\leq L^r - 1$ (e.g., Golomb, 1982). The maximum-length (m-sequence) is obtained when values of c_i are coefficients of an irreducible polynomial of degree r in the Galois field with L elements (see Mamarelis and Marmarelis, 1978). For example, s_k and c_i for binary m-sequences ($L = 2$) assume values of either 0 or 1, and modulo two algebra is used in Eq. (6). Ternary and five-level m-sequences are calculated using algebra modulo three and five, respectively. An m-sequence is uniquely determined by a set of coefficients c_i and the initial content in the register. The sets of coefficients c_i that produce m-sequences of two, three, and five levels can be found in the literature (e.g., Davies, 1970).

M-sequences have a number of properties that are highly desirable in the context of HDR estimation. They are nearly orthogonal to cyclically shifted versions of themselves. Specifically, for any phase of a cyclical shift, binary m-sequences of length n deviate from orthogonality only by $1/n$ (i.e., the scalar product of an m-sequence and its cyclically shifted version deviates from zero by $1/n$). In comparison, an average random sequence deviates from orthogonality by a greater amount, $1/\sqrt{n}$ (e.g., Davies, 1970). Figure 4 shows cyclical autocorrelation functions for sequences of length 511 ($2^9 - 1$) for (A) a random sequence and (B) a binary m-sequence. Note how for this sequence length, the autocorrelation function is zero (away from the zero-shift point) only for the m-sequence. This makes binary m-sequences an ideal means for estimating the impulse response of a system (i.e., the linear component of the system response), since its autocorrelation function approaches delta-function with increasing sequence length: $R_{ss}(k) \xrightarrow{n\to\infty} \delta(k)$.

Ternary and higher-level sequences, however, possess occasional phase values for which the sequences are perfectly anticorrelated. Figure 4C shows how the autocorrelation function for a ternary m-sequence has two phase shifts that are negatively correlated. These phase values must be avoided when constructing multievent sequences.

One cycle of an m-sequence contains all combinations of elements of a subsequence of shift register of

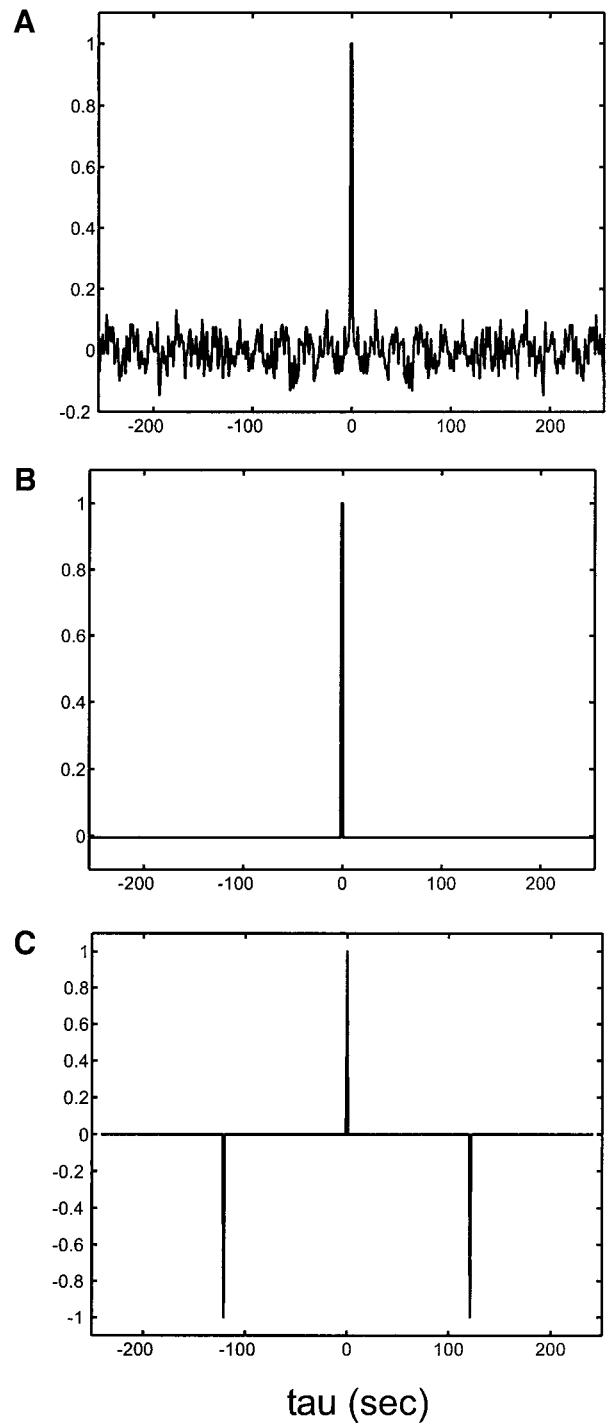

FIG. 4. Cyclical autocorrelation functions for sequences of length 511 ($2^9 - 1$) for (A) a random sequence, (B) a binary m-sequence, and (C) a ternary m-sequence. The autocorrelation functions are normalized so that the peak value is set to 1.

length r except for one. The missing subsequence contains all zeros, which is a cycle in itself (Golomb, 1980). Therefore, combinations (except the all-zeros combination) of event subsequences are nearly perfectly counterbalanced up to the length equal to the order r of an m-sequence. If needed, perfect counterbalancing can be readily achieved by appending a single element to the original sequence (i.e., producing an extended m-sequence). This property is very useful for not only linear systems analysis of HDR responses (Sutter, 1987), but also for exploring nonlinear effects, such as adaptation or expectation (Chen *et al.*, 1996).

The intuitive appeal for using m-sequences in HDR estimation stems from the nature of the design matrix X used for estimation of HDR shape. As seen in Fig. 1, columns of X are shifted versions of the event vector represented in the first column of a sub-matrix for each event type. The efficiency measure E is maximized when the matrix X^TX approaches diagonal matrix (Liu *et al.*, 2001), i.e., when all columns of the matrix X are orthogonal and dot products of each column with itself are maximal. This condition is met if (1) event vectors for each event type are orthogonal to each other and (2) an event vector is orthogonal to a shifted version of itself. M-Sequences satisfy both of these conditions much more closely than average randomly generated sequences.

Data Acquisition for Noise Estimation

For the estimate of noise in HDR estimation efficiency, we used a noise covariance matrix C (see Eq. (3)) calculated from residuals $e = R - X\hat{h}$ using the following fMRI experiment. We obtained fMRI responses in area MT+ from a subject viewing moving stimuli alternating between the lower left and lower right visual quadrants. Stimuli subtended a radius of 10° of visual angle and were centered 12° below the horizontal meridian and 12° to the left or right from the vertical meridian. The stimulus was composed of a circular aperture of upward moving dots (10°/s). Stimuli were presented every 2 s for a duration of 1 s in either the lower left or right quadrants. The visual quadrant was chosen based on a binary m-sequence design. Subjects performed a discrimination task on the moving dots to keep the attentional state at constant level. Low-bandwidth echo-planar images were obtained with a 1.5-Tesla Siemens Vision scanner and a small standard flex coil behind the subject's head (TR = 1 sec, scan duration 512 s, FA 80°, FOV 192 mm).

Noise Estimation from fMRI Data

FMRI time series exhibit a typical temporally-correlated noise pattern with correlation decaying with temporal interval and characterized by correlation time of order 10–15 sec. These essential noise characteristics can be captured by the model used by (Burock and Dale, 2000):

$$c(t) = (1 - a)p^t, \quad \text{for } t > 0, \quad \text{and } c(0) = 1. \quad (7)$$

In order to evaluate the effect of characteristic time-correlated fMRI noise on HDR estimation efficiency, we estimated the noise autocorrelation function from residuals calculated by subtracting from the actual fMRI response, R, an estimate of response $\hat{R}$ reconstructed from the estimated HDR response $\hat{h}$ ($n_h = 12$):

$$err = R - \hat{R} = R - X\hat{h} = R - (X^TX)^{-1}X^TR. \quad (8)$$

Then the estimated noise autocorrelation function was fit by this model after normalizing the peak value to 1. Best fitting model parameters estimated from our fMRI signals in area MT+ were $a = 0.41$, $p = 0.88$. A Toeplitz matrix using the resulting vector, c, was used to generate the noise autocorrelation matrix C. This matrix then was used for calculating HDR estimation efficiencies (Eq. (4)) for both random sequences and m-sequences.

Construction of Event Sequences from M-Sequences

Both single and multievent sequences for erfMRI experiments can be constructed from m-sequences. Although the constructed event sequences are constrained to certain lengths and numbers of event types, the space of m-sequence based designs covers a substantial portion of sequences that are common for erfMRI experiments.

A critical parameter that affects HDR estimation efficiency is the total number of events of a given type in a sequence, which is equivalent to event probability (e.g., Friston *et al.*, 1999; Liu *et al.*, 2001). It has been shown that no-event trials ("zero-events") must be included in order to make HDR response estimation feasible, i.e., the sum of event occurrence probabilities of all event types ought to be $P < 1$ (e.g., Friston *et al.*, 1999). For any random sequence with one event type, the probability of the non-zero event occurrence that maximizes HDR estimation efficiency is $P = 0.5$ (e.g., Liu *et al.*, 2001), which is close to the probability of event occurrence determined by a binary m-sequence $P = (n + 1)/2n$. Therefore, a binary m-sequence can serve for a single-event design "as is," with the constraint that the fMRI signal is sampled $2^r - 1$ times (i.e., the scan duration is $\tau \times 2^r - 1$ s, where τ is the time between temporal samples).

Multievent erfMRI experimental designs can be classified into two types: those that allow the simultaneous occurrence of events of different types (the "overlapping" events design), and designs with mutually exclusive event types (the "nonoverlapping" events design).

For the overlapping events design HDR estimation efficiency is maximized if the probability of each event type is 0.5, as in the case of the single event type. Therefore one can generate a different binary vector $ms_i(t) \in [0,1]$ for each event type independently, where 1 corresponds to event-present interval and 0 corresponds to event-absent interval. For this design there are no restrictions on the number of event types as long as the length of the sequences is $> n_h n_e$.

A straightforward way to use m-sequences for overlapping designs is to cyclically shift the same binary m-sequence for each event type. This m-sequence-based design is similar to that used in electrophysiology experiments of receptive field properties (e.g., Reid *et al.*, 1997). Specifically, let the event vector for event of type 1 be a binary m-sequence of length $n = 2^r - 1$. For all other event types, the same sequence is then shifted by a phase $> n_h$. Figure 5A illustrates how the phase difference between m-sequences representing each event type influences efficiency for 3-overlapping events ($n_e = 3$). To generate the figure, events of type 1 were generated using a binary 6th order m-sequence with parameters $n = 2^7 - 1 = 127$ and $n_h = 12$. Events of type 2 were positioned in time by shifting the original m-sequence cyclically by a fixed phase of $(n + 1)/2 = 64$ steps. Finally, for the third event type, the original m-sequence was cyclically stepped through all phase values. Dips in efficiency at the edges and in the middle of the graph occur when the phase of the third m-sequence comes within n_h steps of either of the first two sequences. These dips occur because for phase differences less than n_h, some columns of matrix X that represent one event type become nearly identical or identical to shifted columns that represent other event types, thus making the matrix $X^T X$ ill-conditioned or singular. Therefore, when designing an erfMRI experiment with overlapping events, one should use cyclical phases that differ, pair-wise, by more than n_h steps.

M-sequences can also be used for more common non-overlapping designs. When the number of events is $L^k - 1$ ($k > 0$), one can create event vectors for each event type by using the following formula:

$$e(t) = \sum_{i=1}^{k} L^i s(t + f_i), \tag{9}$$

where $e(t)$ is an integer indicating the type of the event assigned at the time interval t which ranges from 0 to $L^k - 1$. The phase f_i is added cyclically, with wrap-around modulo n, and is selected empirically to maximize estimation efficiency. Next, an event vector [0,1] for each event type i can be created by assigning 0 for all $e(t) \neq i$, and 1 otherwise.

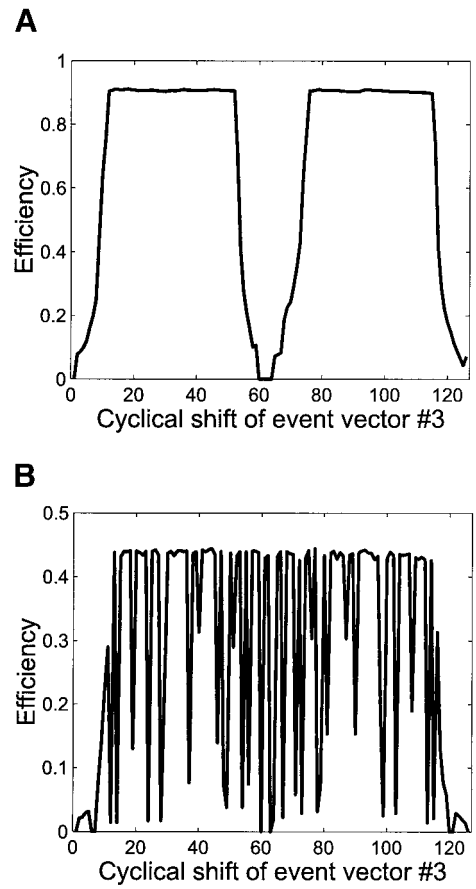

FIG. 5. (A) HDR estimation efficiency (equation 3, with $C = I$), calculated for an experimental design matrix X that uses the same binary m-sequence for 3 overlapping event types. For the second event type the m-sequence is shifted cyclically by the phase of $(n + 1)/2$. For the third event type the m-sequence is cyclically stepped through all n phase values. The dips in efficiency occur where any of the three m-sequences are separated by less than n_h steps. (B) Estimation efficiency as a function of the phase f between two m-sequences used for three-event nonoverlapping design (see Eq. (6)).

For example, if $k = 2$ (thus there are $2^2 - 1 = 3$ event types plus the zero event), the event vector $e(t) \in [0,1,2,3]$ can be constructed from:

$$e(t) = 2*s(t) + s(t + f), \tag{10}$$

where s is a binary m-sequence, and the phase f is selected so as to maximize efficiency. Thus if $n = 7$, $f = 3$, and $s(t) = [0\ 0\ 1\ 0\ 1\ 1\ 1]$ is the chosen m-sequence, then $e(t) = [0\ 3\ 2\ 2\ 1\ 3\ 1]$, which corresponds to the following event vectors for individual event types: $e_1(t) = [0\ 0\ 0\ 0\ 1\ 0\ 1]$, $e_2(t) = [0\ 0\ 1\ 1\ 0\ 0\ 0]$, and $e_3(t) = [0\ 1\ 0\ 0\ 0\ 1\ 0]$.

Intuitively, the reason why the equation (10) affords cases with maximum efficiency (for certain values of f) can be appreciated from the following argument. Since $s(t) \in [0,1]$, Eq. (10) assigns for the i-th time interval t_i an event from either the pair $e(t_i) \in [0,1]$ or $e(t_i) \in [2,3]$.

Since this assignment is governed by an m-sequence, it possesses the property of optimal efficiency E. Likewise, the second term of the equation 10 determines whether the event $e(t_i)$ at time t_i is odd or even. Clearly, this assignment also possesses the property of optimal efficiency when considered independently of the first event assignment. When considered simultaneously, these two assignments interact in a way that results in variable estimation efficiency across phase values f. Figure 5B illustrates the behavior of estimation efficiency as a function of the phase f. Although efficiency drops for $|f| < n_h$, and in addition there are drops in E for multiple values of f, the majority of E values hover around a maximum value of E. Any of these phase values that results in high efficiency can be used for constructing a nonoverlapping erfMRI sequence.

For the nonoverlapping event designs, estimation efficiency is maximized by reaching a tradeoff between maximum-energy for each event type and orthogonality of the column vectors of the design matrix (Liu *et al.*, 2001). For example, in the case of two mutually exclusive events, the optimality condition is given when each event occurs with equal probability of 0.29 (Liu *et al.*, 2001; see also Friston *et al.*, 1999). However, when not only HDR responses but also contrasts between effects are to be estimated, the probability that maximizes estimation efficiency is $1/(n_e + 1)$ (e.g., Liu *et al.*, 2001). We use this formula for determining optimal event probability in efficiency calculations below.

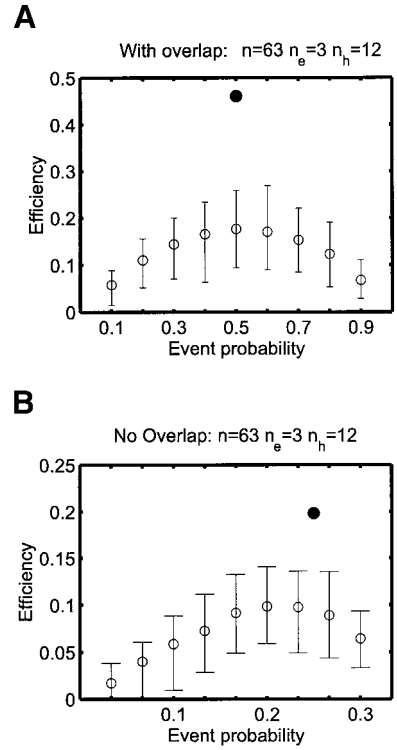

FIG. 6. HDR estimation efficiency as a function of the probability of event. Three equal probability event types are assumed ($n_e = 3$, $n = 63$, $n_h = 12$). Open circles are mean efficiency values, error bars indicate the best and worst efficiencies of 10,000 randomly generated sequences. The filled circle at the top corresponds to the maximal efficiency afforded by an m-sequence-based design. (A) Overlapping-events design. The maximum efficiency occurs for $P = 0.5$. (B) Design with no overlaps (no synchronous events are permitted). The maximum efficiency is achieved for $P < ¼ = 1/(n_e + 1)$.

RESULTS

Comparison of Randomly Generated Sequences and M-Sequences

Figure 6A (open symbols) shows median estimation efficiencies from a sample of 10,000 randomly generated sequences with three overlapping events (plus the zero event) as a function of event probability. For each probability value, the number of events is equal across event types. The length of the sequence, n, is 63, and the length of the HDR, n_h, is 12. Error bars indicate the best and the worst values from each sample. No temporal correlation in the noise is assumed. It can be seen that maximal median efficiency is achieved for a probability of 0.5.

The filled circle indicates the estimation efficiency of the m-sequence. For this particular choice of parameters, the m-sequence has more than twice the efficiency of the median random sequence. The best random sequence approaches only within <75% of the m-sequence efficiency, suggesting that achieving a maximally efficient sequence through random search is computationally impractical.

Figure 6B illustrates how HDR estimation efficiency behaves as a function of event probability for three *non*overlapping events, assuming probabilities are equal for all events (conventions as for Fig. 6A). The event-probability for achieving maximal efficiency is slightly lower than 0.25. Despite the fact that an optimal m-sequence design is constrained to $P = 0.25$, and thus deviates slightly from optimal probability, the efficiency achieved by m-sequences (indicated by the closed circle; event vectors generated using Eq. (10)) is substantially higher than that afforded by random sequences.

Figure 7 summarizes HDR estimation efficiency for designs using a single event type as a function of sequence length. The left column (Figs. 7A and 7C) plots efficiencies for HDR length, $n_h = 12$, and the right column (Figs. 7B and 7D) plots efficiencies for $n_h = 24$. The error bars in the graphs of the top row (Figs. 7A and 7B) indicate the best and worst efficiencies of the 10,000 randomly generated event sequences. Asterisk symbols indicate the efficiency of the m-sequence. Efficiency grows with sequence length for both m-sequences and randomly generated sequences.

The advantage of m-sequences over random sequences is greatest for short sequences. This is more

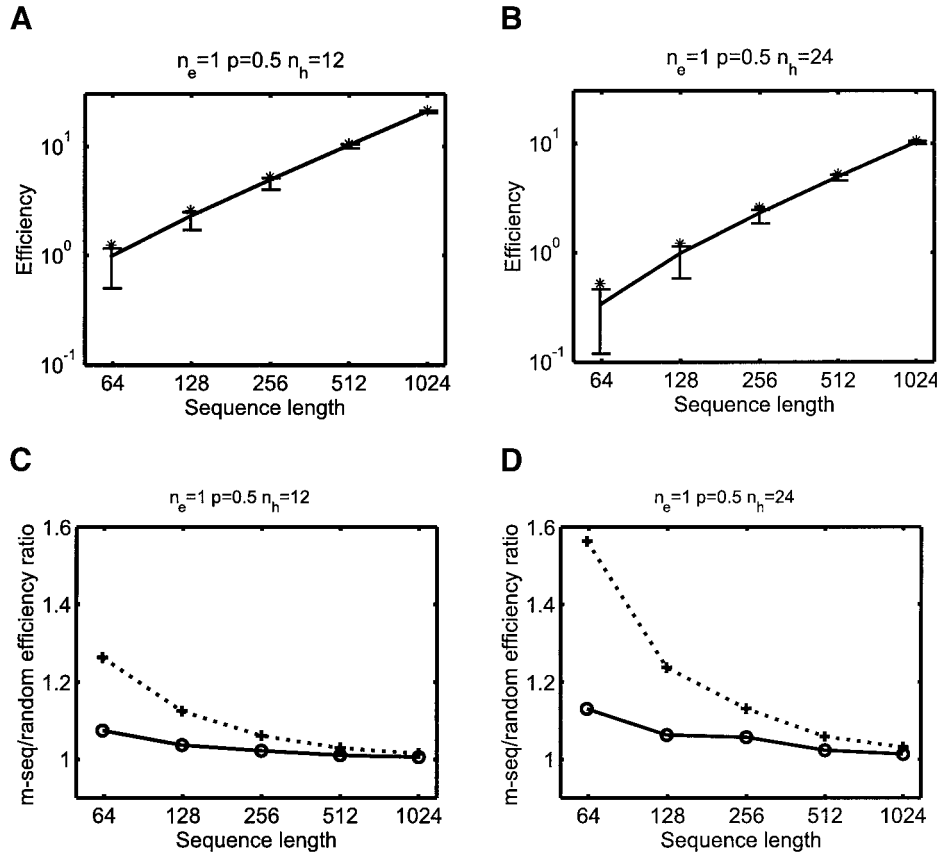

FIG. 7. Top row (A, B): Estimation efficiency as a function of sequence length n for experiments with one event type for $n_h = 12$ (A) and $n_h = 24$ (B). The continuous line indicates the median efficiency of random designs, and the error bars indicate the best and the worst efficiencies generated after 10,000 iterations. Bottom row (C, D): ratios of the estimation efficiency of m-sequence-based design to the best random sequence obtained after 10,000 iterations (continuous line) and to the median random design efficiency (dotted line) for $n_h = 12$ (C) and $n_h = 24$ (D).

clearly seen in Figs. 7C and 7D that plot the results in Figs. 7A and 7B as the ratio of the efficiency of the m-sequence over efficiencies of the randomly generated sequences. Dotted lines indicate ratios with respect to the median of the random sequences, and solid lines indicate ratios with respect to the most efficient random sequence. It is clear from these ratios that for short sequences, choosing the best of 10,000 sequences improves efficiency dramatically over a typical random sequence, but the best sequence is still not as efficient as the m-sequence. For long sequences, the efficiency of the random sequence approaches, but never exceeds the efficiency of the m-sequence-based design, because event subsequences are naturally more counterbalanced for longer sequences. In addition, designs that sample HDR with more sampling points (c.f., Figs. 7C and 7D) offer greater benefit in efficiency of m-sequence-based designs.

We have also calculated the ratio of m-sequence efficiency to the most efficient of 100,000 and one million randomly generated sequences ($n_h = 24$, $n = 63$ and 127). Increasing to 100,000 sequences, efficiency of the best random sequence improved only by 1.8% ($n = 63$), and 0.67% ($n = 127$). After 1 million sequences the efficiency of the best random sequence improved only by another 1.4% and was still below that afforded by an m-sequence by 15%. This remarkably insignificant improvement after 100-fold increase in computational time illustrates how difficult it is to reach m-sequence efficiency by random search.

The advantage of m-sequences over random sequences in HDR estimation efficiency is even greater for designs that use more than one event type. Figure 8 plots efficiency ratios for designs employing three event types (convention as in Figs. 7C and 7D). Top row (Figs. 8A and 8B) plots efficiency ratios for three overlapping events, and the bottom row (Figs. 8C and 8D) shows efficiency ratios for three nonoverlapping events. Left and right columns, as in Fig. 6, correspond to HDRs with $n_h = 12$ and $n_h = 24$ sampling points respectively. Note that for $n_h = 24$ (Figs. 8B and 8D) efficiency ratios are absent for the shortest sequence length ($n = 63$), since the efficiency is zero for m-sequence-based designs when $n < n_h n_e = 72$.

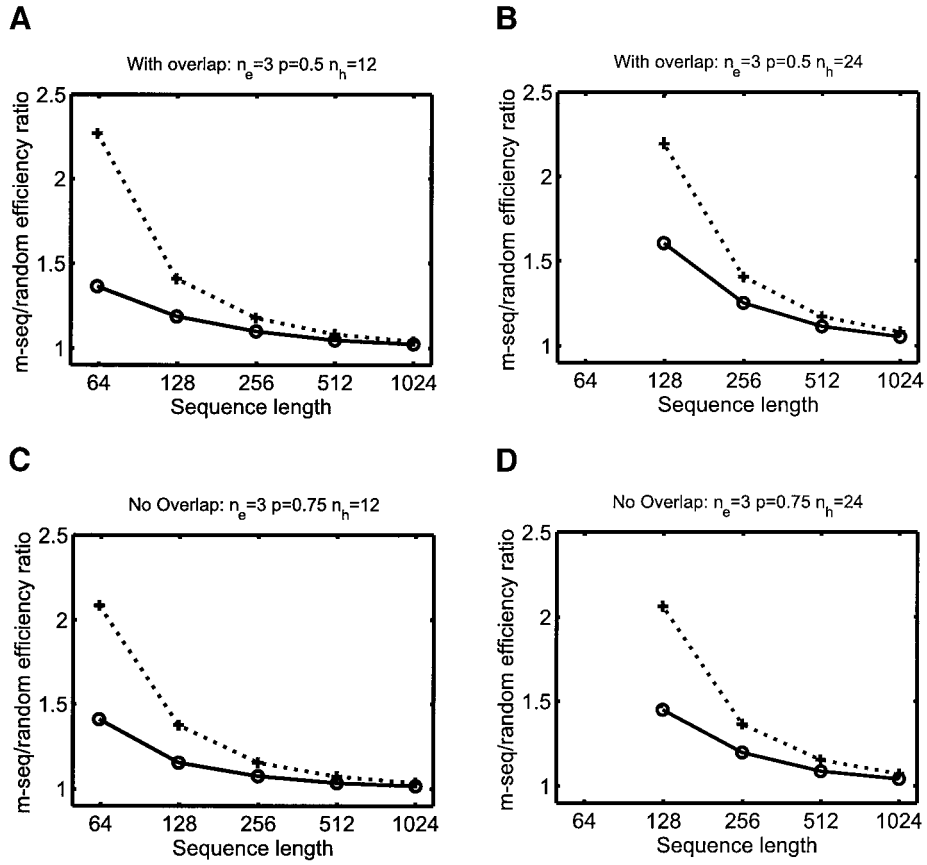

FIG. 8. Ratios of m-sequence-based estimation efficiency to that of random design for three event types. Top row (A, B): overlapping event design; bottom row (C, D): nonoverlapping events design. Left column (A, C): $n_h = 12$, right column (B, D): $n_h = 24$. Conventions as described in the legends of Figs. 6C and 6D.

Efficiency ratios are greater for 3 event types than for one event type (c.f. Figs. 7 and 8). This is because the fraction of random sequences that exceed a criterion level of efficiency decreases with the number of event types, so the probability of finding such a sequence by chance is lower for $n_e = 3$ than for $n_e = 1$.

M-sequence designs used for Figs. 5, 6, and 7 employed either single (Fig. 7) or combinations (Figs. 6 and 8) of binary m-sequences. The results are similar for nonbinary m-sequences. Figure 9 plots efficiency ratios for non-overlapping designs using ternary (3-level, Fig. 9A) and 5-level (Fig. 9B) m-sequences. As in previous examples, m-sequence based designs afford unequivocal advantage over random-sequence designs. The relationship between the efficiencies of the m-sequence and the random sequences is similar to the overlapping designs: the greatest advantage of m-sequence occurs for shorter sequences and more event types.

Effect of Noise on Estimation Efficiency

Next, we explored how knowledge of the fMRI noise autocorrelation parameters influences estimation efficiency of random vs m-sequence-based designs. Each scatterplot in Fig. 10 shows estimation efficiencies calculated without noise information (x-axes) (i.e., $C = I$) vs efficiencies with fMRI noise autocorrelation (y-axes). Closed symbols show efficiencies for 1000 random sequences of length 127 (Figs. 10A and 10C) and 511 (Figs. 10B and 10D) and for 1 event (Figs. 10A and 10B) and three overlapping events (Figs. 10C and 10D). An open circle indicates the efficiency of an m-sequence-based design using phase shifts that maximize efficiency without noise. Estimation efficiency in the presence of correlated noise systematically exceeds that of in its absence. This is expected since correlated noise is more predictable than uncorrelated noise and thus information about it can be used for noise suppression.

Distributions along the x-axis of each plot show the advantage in efficiency of m-sequences over random sequences when noise is assumed to be i.i.d. (as also shown in Figs. 7A and 7B). When noise, more realistically, is assumed to be correlated in time, efficiency of some random sequences exceeds the efficiency of an m-sequence-based design. High efficiency can be

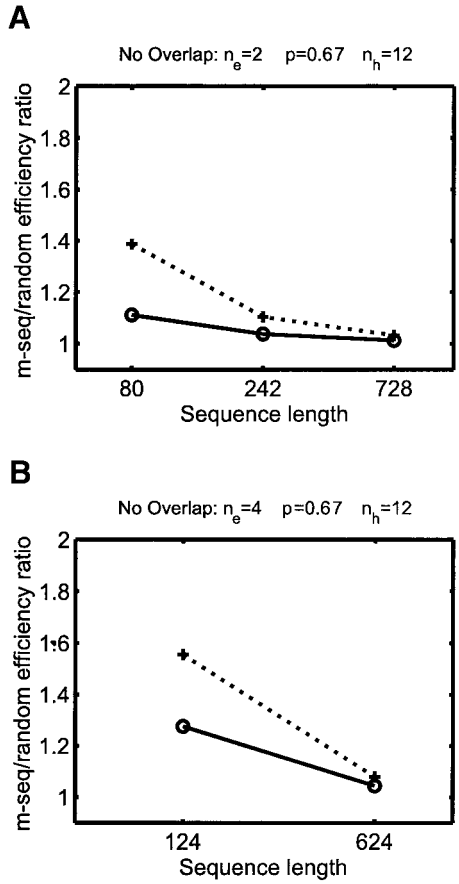

FIG. 9. Ratios of m-sequence-based estimation efficiency to that of random sequences for designs that use nonbinary m-sequences. (A) Efficiency ratios for designs with two event types. Ternary m-sequences are used. (B) Efficiency ratios for designs with four event types. Five-level m-sequences are used. Conventions as described in the legends of Figs. 6C and 6D.

achieved for random sequences with correlated noise because the experimental design matrix X can act as a whitening matrix with respect to the inverse of the noise correlation matrix X: $X^T C^{-1} X$ (c.f. Eq. (5)).

This decorrelation effect on some random sequences is maximal when there is one event type and sequences are relatively long (Fig. 10B). As the number of event types increases, the advantage offered by m-sequences increases. For three non-zero event types, m-sequences offer higher efficiency than the random method, even after taking into account noise (Figs. 10C and 10D). As in the case without noise, the advantage of m-sequences is greatest for shorter sequences (c.f. Figs. 10C and 10D). Finally, the decorrelation effect exhibited by some random sequences of one event-type cases is weaker for designs that use non-truncated design matrices: scatterplots in Figs. 10E and 10F replot efficiencies using parameters of Figs. 10A and 10B, respectively, albeit for nontruncated design. Note that for n = 127 the advantage of random sequences is substantially reduced (c.f. Figs. 10A and 10E), while for n = 511, the reduction is lesser (c.f. Figs. 10B and 10F).

Computational Complexity of Random Search vs M-Sequences

In principle, it is possible to generate an m-sequence by chance using the random search algorithm, but the probability of this is extremely small. For example, there are 16 shift register values of order 8 that would generate a binary m-sequence of length n = 255 (Davies, 1970). Since a cyclically shifted m-sequence is also an m-sequence, this would make a total of 4080 different m-sequences. Considering that there are $2^{255} \approx 10^{80}$ binary sequences of length 255, it is quite unlikely that an experimenter would produce an m-sequence by chance.

However, not all sequences that afford high estimation efficiency are m-sequences. An alternative approach to estimating the likelihood of generating ran-

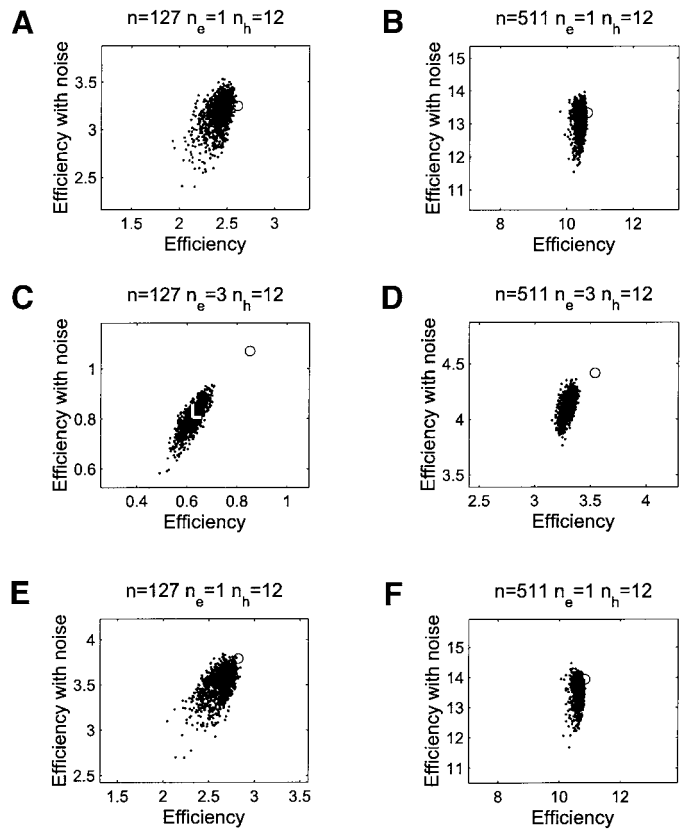

FIG. 10. Comparison of estimation efficiencies for the case when noise is unknown (i.e., $C = I$; plotted on x-axis) with the case when the noise covariance is known (y-axis). Dots plot efficiencies for 1000 randomly generated sequences. An asterisk indicates efficiency for an m-sequence-based design. (A, B) one event type (n_h = 12); (C, D) three event types (n_h = 12). White bars in (C) indicate one standard deviation of the distribution of efficiencies in each dimension. (E, F) Same as A, B, but in this case the design matrix X was composed of canonical nontruncated convolution matrices.

dom sequences with efficiency close to that afforded by m-sequences is to consider the distribution of efficiencies of random sequences. Figure 10 gives some idea about this distribution: it is highly skewed for designs that use a single event type and long event sequences (e.g., see Fig. 10B). For short random sequences with many event types efficiency distribution approaches normal distribution (see Fig. 10C). In this case we can estimate the probability of generating a random sequence above some criterion efficiency by assuming a normal distribution. White bars in Fig. 10C indicate one standard deviation in each dimension. These bars meet at the mean, which is exceeded by the m-sequence-based efficiency by 6.7 standard deviations when the noise is not accounted for (x-axis), and 5.2 standard deviations when the noise autocorrelation is known (y-axis). Assuming a Gaussian distribution and parameters identical to those used in Fig. 10C ($n = 127$, $n_h = 12$, $n_e = 3$), the probability of generating such an efficient sequence randomly is $P = 10^{-11}$ for the case when noise autocorrelation is not known (for parameters in Fig. 10D, i.e., $n = 127$, $n_h = 12$, $n_e = 3$, $p \approx 3 \cdot 10^{-10}$). Therefore, it appears impractical to attempt to reach efficiency afforded by m-sequences by random search.

This conclusion is reinforced by our simulations using 10,000; 100,000; and 1 million randomly generated sequences with parameters: $n = 63$, $n_h = 12$, $n_e = 1$. Each increase in the number of generated sequences by an order of magnitude improved random sequence performance by less than 2%. This is consistent with a distribution of efficiencies from the family of exponential distributions, which support our estimates above based on a Gaussian distribution.

DISCUSSION

We introduce the m-sequence to event-related FMRI as a computationally efficient method for generating stimulus sequences that maximize the ability to estimate the hemodynamic response function to a given event. We show that the standard approach of searching for the best randomly generated sequence is not practical for experimental designs where high estimation efficiency is essential. Specifically, m-sequence-based experimental designs afford substantial HDR estimation efficiency when the scan duration is relatively short, and for multiple event types. M-sequences are especially useful if the multi-event design allows for overlapping, or simultaneous occurrences of several events of different types.

Why do m-sequences tend to outperform random sequences in terms of HDR estimation efficiency? Liu *et al.* (2001) derive an upper bound on estimation efficiency for the independent identically distributed Gaussian noise model (i.e., $C = \sigma^2 I$). They show that the maximum efficiency condition is met when eigenvalues of matrix $X^T X$ are all equal. This leads to a requirement that maximum efficiency design matrices ought to achieve optimal balance between maximizing the energy in each of the columns of the design matrix X and reducing correlation between the columns. Indeed, m-sequence-based designs meet both of these criteria. First, they contain equal numbers of events such that energy for each event is maximized. Second, columns of the design matrix approach mutual orthogonality. Exact orthogonality is achieved only between first columns of each convolution submatrix. As the columns shift within convolution submatrices, exact orthogonality property is lost, but columns still remain weakly correlated. Indeed, casual inspection of eigenvalues of $X^T X$ matrix (not shown) reveals that most eigenvalues for m-sequence designs tend to be identical, while eigenvalues for random designs vary widely and range nearly-smoothly over the spanned interval.

We show herein that if the correlated noise were exactly known, one could select random sequences that result in estimation efficiency superior to m-sequence-based designs for cases of one event type (or two event types with very long event sequences). This is so because there exist random sequences that result in design matrix X, which effectively decorrelate (the inverse of) noise covariance matrix. The fact that fMRI noise varies not only across subjects and scanners, but also across and within experimental runs, makes it impractical to design high-efficiency random-sequence-based experiments that incorporate a perfect model of noise properties. Therefore, in the circumstances of unknown noise, m-sequences afford designs with superior estimation efficiency. Moreover, for designs that use more than one event type, the contribution of noise information becomes inessential, as it does not help random sequences to reach the efficiency afforded by m-sequences.

We have constrained our analysis to truncated design matrices that are consistent with discontinuation of scanning once the stimulus presentation sequence is completed. We have chosen this design since it maximizes estimation efficiency per unit of scan time. Extending scanning duration for additional n_h sampling points increases estimation efficiency albeit at a price of increased scan duration. The choice of truncated vs nontruncated design matrix does not affect our results. In fact, our simulations indicate that the m-sequence advantage over random sequences tends to increase for nontruncated designs. Furthermore, the decorrelation effect exhibited by some random sequences for one event-type designs is substantially reduced for nontruncated designs (see Figs. 10E and 10F).

However, high efficiency afforded by m-sequences comes at a price of constraints associated with the nature of those sequences. One constraint in using m-sequences is that m-sequence experimental designs are restricted to a set of sequence lengths. These lengths are always $L^r - 1$, where the number of levels,

L, is a prime integer (in practice, L = 2, 3, or 5) and the order r is an integer. However, the available lengths span a broad range of values that cover a substantial set of lengths that are routinely used in erfMRI experiments.

Another constraint is that for non-overlapping events, the number of event types is restricted to m-sequence designs that use $L^k - 1$ event types (excluding the zero-event). For example, nonoverlapping m-sequence designs can be generated by means of equation 9 with 1 ($L = 2$, $k = 1$), 2 ($L = 3$, $k = 1$), 3 ($L = 2$, $k = 2$), 4 ($L = 5$, $k = 1$), 7 ($L = 2$, $k = 3$), 8 ($L = 3$, $k = 2$), 15 ($L = 2$, $k = 4$), and 26 ($L = 3$, $k = 3$) event types, but not with 5, 6, 9, etc. event types. Fortunately, the list of available nonoverlapping designs covers a large portion of designs typically used in fMRI experiments. Moreover, these constraints are not applicable for overlapping-events designs.

It has been shown that HDR estimation efficiency is highest for a hybrid block-ER design where event occurrence probability slowly varies across time (e.g., Liu *et al.*, 2001). M-sequence based designs achieve optimal efficiency under a stringent requirement of constant event probability for the duration of an experimental run. These designs might be thus preferable for studies that are sensitive to expectation, neuronal adaptation, and priming effects.

Finally, data acquired during experiments using m-sequences lends to a computationally efficient linear (Sutter, 1987; Bernadette and Victor, 1994) and nonlinear systems analysis (Chen *et al.*, 1996).

The code for generation of m-sequences and calculation of estimation efficiency is available online at: http://www.cnl.salk.edu/~giedrius/professional/m-seqs/msequences.htm.

ACKNOWLEDGMENTS

We are indebted to Tom Liu and anonymous reviewers for valuable comments. Supported by NIH Grant 521743.

REFERENCES

Bernadette, E. A., and Victor, J. D. 1994. An extension of the m-sequence technique for the analysis if multi-input nonlinear systems. In *Advanced Methods of Physiological System Modeling* (V. Z. Marmarelis, Ed.), Vol. 3, pp. 87–110. Plenum Press, NY.

Boynton, G. M., Engel, S. A., Glover, G. H., and Heeger, D. J. 1996. Linear systems analysis of functional magnetic resonance imaging in human V1. *J. Neurosci.* **16:** 4207–4221.

Burock, M. A., Buckner, R. L., Woldorff, M. G., Rosen, B. R., and Dale, A. M. 1998. Randomized event-related experimental designs allow for extremely rapid presentation rates using functional MRI. *Neuroreport* **9:** 3735–3739.

Burock, M. A., and Dale, A. M. 1998. Estimation and detection of event-related fMRI signals with temporally correlated noise: A statistically efficient and unbiased approach. *Hum. Brain Mapp.* **11:** 249–260.

Chen, H.-W., Aine, C. J., Best, E., Ranken, D., Harrison, R. R., Flynn, E. R., and Wood, C. C. 1996. Nonlinear analysis of biological systems using short m-sequences and sparse-stimulation techniques. *Ann. Biomed. Eng.* **24:** 513–536.

Dale, A. M. 1999. Optimal experimental design foe event-related fMRI. *Hum. Brain Mapp.* **8:** 109–114.

Dale, A. M., and Buckner, R. L. 1997. Selective averaging of rapldly presented individual trials using fMRI. *Hum. Brain Mapp.* **5:** 329–340.

Davies, W. D. T. 1970. *System Identification for Self-Adaptive Control*. Willey-Interscience, London/New York/Sidney/Toronto.

Fize, D., Boulanouar, K., Chatel, Y., Ranjeva, J.-P., Fabre-Thorpe, M., and Thorpe, S. 2000. Areas involved in rapid categorization of natural images: An event-related fMRI study. *Neuroimage* **11:** 634–643.

Friston, K. J., Zarahn, E., Josephs, O., Henson, R. N., and Dale, A. M. 1999. Stochastic designs in event-related fMRI. *Neuroimage* **10:** 607–619.

Golomb, S. W. 1982. *Shift Register Sequences*. Aegean Park Press, Laguna Hills, CA.

Hinrichs, H., Scholz, M., Tempelmann, C., Woldorff, M. G., Dale A. M., and Heinze, H. J. 2000. Deconvolution of event-related fMRI responses in fast-rate experimental designs: Tracking amplitude variations. *J. Cogn. Neurosci.* **8**(Suppl. 2): 76–89.

Josephs, O., and Henson, R. N. 1999. Event-related functional magnetic resonance imaging: Modelling, inference and optimization. *Phil. Trans. R. Soc. Lond. B* **354:** 1215–1228.

Kay, S. M. 1993. *Fundamentals of Statistical Signal Processing: Estimation Theory*. Prentice-Hall PTR.

Liu, T. T., Frank, L. R., Wong, E. C., and Buxton, R. B. 2001. Detection power, estimation efficiency, and predictability in event-related fMRI. *Neuroimage* **13:** 759–773.

Marmarelis, P. Z., and Marmarelis, V. Z. 1978. *Analysis of Physiological Systems*. Plenum Press, New York/London.

Reid, R. C., Victor, J. D., and Shapley, R. M. 1997. The use of m-sequences in the analysis of visual neurons: Linear receptive field properties. *Vis. Neurosci.* **14:** 1015–1027.

Rosen, B. R., Buckner, R. L., and Dale, A. M. 1998. Event-related functional MRI: Past, present, and future. *Proc. Natl. Acad. Sci. USA* **95:** 773–780.

Sutter, E. E. 1987. A practical nonstochastic approach to nonlinear time-domain analysis. In *Physiological Systems Modeling* (V. Z. Marmarelis, Ed.), Vol. 1, pp. 303–315. University of Southern California.